Polymer Vol. 37 No. 13, pp. 2695–2700, 1996

0032-3861/96/$15.00 + 0.00

Study of dye diffusion in polymers using Rutherford backscattering

T. E. Shearmur*, D. W. Drew, A. S. Clough and M. G. D. van der Grinten
Department of Physics, University of Surrey, Guildford, Surrey GU2 5XH, UK

and A. T. Slark
ICI Imagedata, Brantham, Manningtree, Essex CO11 1NL, UK
(Received 28 September 1995; revised 14 November 1995)

Rutherford backscattering has been used to study dye diffusion (using a sulfur atom in the dye as a label) into various polymer films with different glass transition temperatures. Diffusion into the films is induced via dye diffusion thermal transfer printing. Backscatter spectra are initially transformed into depth profiles, which are then fitted to the relevant equations in order to obtain diffusion coefficients. Both the diffusion coefficients and the depth of penetration of the dye are found to be controlled by the glass transition of the acceptor polymer matrix. With the dye–polymer interactions being similar in all samples and independent of polymer glass transition temperature, the diffusion coefficients are seen to be in excellent agreement with free-volume theories of diffusion. Backscatter specta are compared to theoretical simulations to obtain mass fractions for the dye/matrix throughout the polymer film. Copyright © 1996 Elsevier Science Ltd.

(Keywords: dye diffusion; polymer films; Rutherford backscattering)

INTRODUCTION

Dye diffusion thermal transfer printing is a method for producing high-quality continuous-tone colour images from an electronic source[1]. The process involves the transfer of dye from a donor ribbon to an acceptor sheet, which are brought into intimate contact at high temperature and pressure. Heat is supplied to the back of the donor ribbon via contact with a thermal head, consisting of an array of electronically controlled heating elements, which are separately controlled to enable spatial resolution. The quantity of dye transferred depends on the temperature reached during printing. The temperature of dye transfer and the print time vary, but are typically 250°C and 12 ms respectively. Images are produced by the sequential transfer of dye from yellow, magenta and cyan panels, which are repeated in series along the length of the ribbon. Different colours are produced by controlling the relative amounts of yellow, magenta and cyan dye transferred at each pixel.

Both the donor and acceptor sheets are multilayer structures, but the dye transfers from a polymer coating in the donor sheet to an acceptor polymer coating in the receiver sheet. It has been shown that the mechanism for dye transfer is diffusion between polymers rather than sublimation[2]. Therefore, the dye transfer process can be viewed as permeability from a donor polymer to an acceptor polymer where the temperature of transport is above the glass transition temperatures of both the donor and the acceptor matrices. The dye transfer process has been modelled previously. Hann and Beck[1] illustrated that the use of a model involving diffusion and partition coefficients was reasonable in predicting the dye transfer. More recently, Shinozaki and Hirano[3] have proposed a mechanism involving adsorption followed by diffusion. In both cases, it has been proposed that the depth of penetration of the dye in the receiver layer is of the order of micrometres but, to our knowledge, this has not been determined experimentally.

The determination of the distribution of a solute in a polymer within a surface layer of less than several micrometres is an interesting problem for surface analysis. Both X-ray photocorrelation spectroscopy and secondary ion mass spectrometry have been widely used as tools in the surface analysis of polymers, but the analysis is limited to depths of <100 Å (ref. 4). Attenuated total reflection (a.t.r.) spectroscopy is an infra-red spectroscopic method that can be used for the analysis of thicker specimens[5], but the surface resolution (approximately 0.5 μm) makes it unsuitable for this study. In principle, neutron reflection could be used, but there are two problems: the requirement for calibration with another technique, and the need for isotopic labelling[6]. The latter can be expensive and may produce materials with properties that differ from those actually of interest. Rutherford backscattering (RBS) is a surface analysis tool that involves bombarding a target with accelerated ions under vacuum and observing them after they have suffered elastic collisions in the target and are scattered at an angle greater than 90° (ref. 7). It is a technique that can analyse the elemental composition of surfaces in the micrometre range with excellent resolution and sensitivity. It is ideal when searching for a heavy element (even at low concentrations) in a matrix composed of lighter elements.

---

* To whom correspondence should be addressed

This paper describes the use of Rutherford backscattering for the determination of the distribution of dye molecules in polymer matrices, where all polymers consist of carbon, hydrogen and oxygen only, but where the dye contains a sulfur atom, which can be used as a label. The dye/polymer matrices were created using dye diffusion thermal transfer printing with polymers of varying glass transition temperatures as acceptor matrices.

EXPERIMENTAL

Materials used

The dye used for this study is a heterocyclic azo dye whose composition is illustrated in *Figure 1*. The dye molecule predominantly consists of carbon, hydrogen, oxygen and nitrogen but contains one sulfur atom, which was used as the tracer element for the RBS analysis. Various polymers were used as acceptor layers for the dye diffusion. They were all amorphous, containing carbon, hydrogen and oxygen only. Glass transition temperatures were measured using a Perkin-Elmer DSC-4 differential scanning calorimeter using a heating rate of 20°C min^{-1} and calibrated using an indium standard. The polymers used are given in *Table 1* together with their glass transition temperatures (T_g) and solubility characteristics. Solubility parameters (δ) were calculated using the method given by Fedors[8,9] according to the equation:

$$\delta = (E_{\mathrm{coh}}/V)^{1/2} \tag{1}$$

where E_{coh} is the cohesive energy and V is the volume of the dye molecule or of the polymer repeat unit respectively. Both quantities were calculated from group contributions listed in the review by Van Krevelen[9]. The difference $\delta_d - \delta_p$ between the solubility parameters of the dye (δ_d) and of the polymer (δ_p) provides a measure of the dye/polymer compatibility. This is discussed in more detail later on.

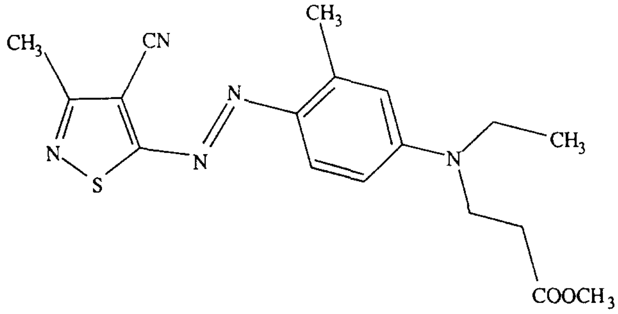

Figure 1 Structure of heterocyclic azo dye solute. The solute contains sulfur, which acts as a label for the RBS experiments

Creation of dye/polymer blends

Donor sheets are created using the dye and a polymeric binder. The dye is mixed with poly(vinyl butyral) (PVB) (1/2 w/w) and dissolved in tetrahydrofuran (THF) solvent. Thin (6 μm) poly(ethylene terephthalate) (PET) base films containing thermally resistant sheets on the rear side are coated with this mixture to create donor films. The PET base is coated using a wire bar to produce a thickness of 1 μm and immediately dried using a hair-drier. The transformation from dilute to solid solution is rapid (<1 s), yielding a supersaturated solution of dye in polymer. Samples are then placed in an oven for 30 s at 110°C. This treatment was shown to be effective in reducing THF to negligible proportions without causing the dye to phase-separate. The dye coat layer is then supercoated with a thin 0.05 μm layer of poly(hydroxypropylmethyl cellulose) (Methocel E50, obtained from Dow Chemical Co.). This layer is required to prevent adhesion between the dye coat and receiver layers whilst at high temperature and pressure, during the thermal transfer printing process.

The polymers listed in *Table 1* are used as acceptor layers. They are dissolved in THF solvent and a wire bar is used to coat 125 μm thick sheets of PET with the solution, to create receiver sheets. The resulting polymer layers are 4 μm thick. The coatings are then dried by placing the receiver sheet in an oven at 140°C for 3 min.

The donor sheet and receiver sheet are placed with the donor and acceptor layers in intimate contact. The transport of dye is induced using a thermal transfer printer with a constant print time. After printing, the donor and receiver sheets are separated, to produce polymer sheets containing a constant amount of dye across the printed surface.

Rutherford backscattering (RBS) measurements

RBS experiments are performed with a beam of 2 MeV $^4\mathrm{He}^+$ ions at the Van de Graaff accelerator of the University of Surrey. Samples of film of 1 cm^2 are cut from receiver sheets into which dye had been transferred.

Table 1 Characteristics of polymers used as dye acceptor layers

Polymer type	Glass transition T_g (°C)	Solubility, δ_p ((J $\mathrm{cm}^{-3})^{1/2}$)	Solubility difference, $\delta_d - \delta_p$ ((J $\mathrm{cm}^{-3})^{1/2}$)
A Polyester[a]	47	24.1	0.7
B Polyester[b]	67	24.7	0.1
C Polyester[c]	71	24.6	0.2
D Poly(vinyl butyral)[d]	85	23.0	1.8
E Polyester[e]	100	23.5	1.3

[a] Polyester **A**: 'Vylon103' (Toyobo), 20% isophthalic acid, 25% terephthalic acid, 5% sebacic acid, 25% neopentyl glycol, 25% ethylene glycol
[b] Polyester **B**: 'Vylon 200' (Toyobo), 25% isophthalic acid, 25% terephthalic acid, 25% neopentyl glycol, 25% ethylene glycol
[c] Polyester **C**: 'Vylon 290' (Toyobo), 25% isophthalic acid, 25% terephthalic acid, 30% ethylene glycol, 20% dihydroxyethyl bisphenol A
[d] Poly(viny butyral) **D**: 'PVB-BX1' (Sekisui), 5% vinyl acetate, 35% vinyl alcohol, 60% vinyl butyral
[e] Polyester **E**: 'Dynapol L912' (Dynamit-Nobel), 50% terephthalic acid, 50% cyclohexane dimethanol

The back of each film is attached to a slightly larger, thin aluminium plate using double-sided adhesive tape. The dye/polymer surface is then carbon coated to a thickness of a few tens of angstroms by vacuum deposition and silver dag applied at the edge of the film. This provides an electrical contact between the film surface and the aluminium plate to prevent charge build-up and sparking. The aluminium plate is mounted in a steel target holder located at the bottom of a rotatable liquid-nitrogen-containing cylinder, in the centre of an evacuable target chamber. The vacuum in the chamber is typically of the order of 10^{-6} Torr and spectra are acquired in 10–15 min. The beam current through the sample is monitored continuously to make sure it does not exceed 2 nA in order to minimize any beam heating effects. The beam size is approximately 9 mm^2 to cover a large number of pixels, thereby producing an averaged spectrum. Sample changes are performed in approximately 5 min via a load lock. A triple-alpha source (^{239}Pu, ^{241}Am, ^{244}Cm) is mounted in the chamber for calibration purposes.

The energy of particles scattered at angles greater than 90° is invariably lower than that of the incoming particles and the kinematic factor (K) relates the scattered particle energy to the incident particle energy. At a particular scattering angle, K is determined solely by the projectile and target masses. Backscattered particles are detected in a 100 μm thick silicon surface Ortec CA-11-50-100 detector placed at an angle of 165° to the incident beam. The signal is then routed through a preamplifier (Ortec 142) and an amplifier (Ortec 671) before being recorded on a 2048-channel Ortec Ace multichannel analyser. If elements were only present at the extreme surface, the energy spectrum of the backscattered particles would show a series of peaks. However, since the elements generally have a depth distribution and the incident ions lose energy as they penetrate the target, the spectrum exhibits a series of broad continua corresponding to the depth distribution of the elements present. All polymer matrices contain C, O and H only, but the dye consists of C, O, H, N and S. Hence, analysis of the sulfur depth distribution determines the dye distribution.

RESULTS AND DISCUSSION

Dye diffusion profiles and diffusion coefficients

Figure 2 illustrates a typical spectrum of the sulfur diffusion profile in a target containing carbon and oxygen. The carbon and oxygen edges and the triple-alpha peaks (used for calibration) are clearly visible. The sulfur edge is just visible on the global spectrum but can be seen more clearly in the inset. The sulfur spectra are converted to depth concentration profiles by converting the channel/energy scale to a depth scale and correcting the yield to account for the energy dependence of the reaction cross-section[7,10,11]. The first objective is achieved by calculating the approximate atomic composition of the targets and the ranges of helium ions in the target materials using TRIM[12], a program incorporating the stopping powers calculated by Ziegler *et al.*[13]. A typical depth concentration profile is illustrated in *Figure 3*. If it is assumed that the dye diffusion thermal transfer printing process can be described as a species diffusing from a source that holds the surface at a fixed concentration into a semi-infinite layer, the diffusion equation can be described by[14]:

$$y = A\,\mathrm{erfc}[x/(4Dt)^{1/2}] \tag{2}$$

where A is a constant, x is the depth, D is the diffusion coefficient and t is the time during which diffusion takes place. This equation is convoluted with a Gaussian (f.w.h.m. 0.2 μm) to take the system resolution into account and fitted to the depth profiles. *Figure 3* shows an example of the fits produced.

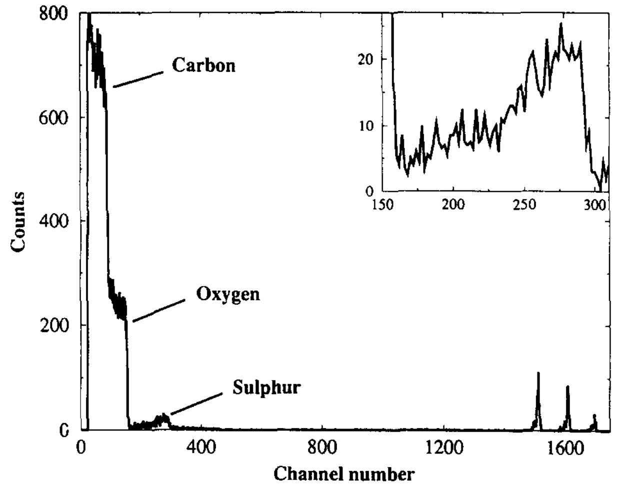

Figure 2 Typical RBS spectrum of heterocyclic azo dye in acceptor polymer matrix. The carbon and oxygen edges and the triple-alpha peaks used for calibration are clearly shown. The sulfur edge is just visible on the global spectrum and is highlighted in the inset

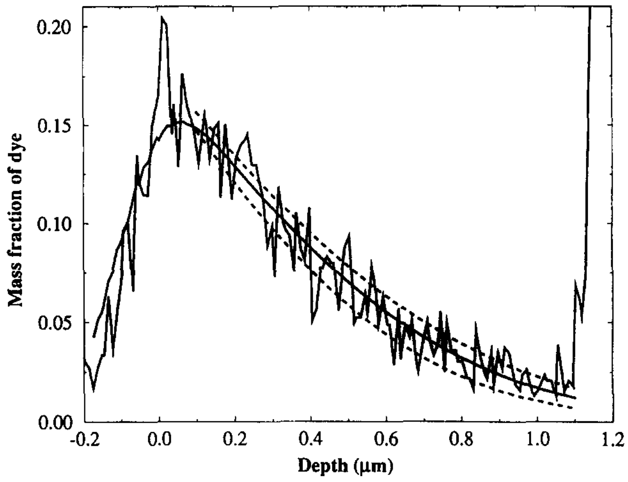

Figure 3 Dye diffusion profile in acceptor polymer **D** with best fit of equation (2). The print time was 12.7 ms and the diffusion coefficient was found to be 1.56×10^{-7} cm^2 s^{-1}. The dashed lines above and below the fit correspond to different diffusion coefficients $D \pm 20\%$, chosen to encompass the data. These were used as estimates of the error on the best-fit value obtained from the fitting program

Results for the diffusion coefficient and depth of penetration of the heterocyclic azo dye in various polymers are given in *Table 2*. The errors stated in the table are calculated from the estimated errors to each fit and from the spread of values obtained for different runs with the same sample. It is clear that both the diffusion coefficient and, therefore, the depth of penetration of the dye decrease as the acceptor polymer T_g increases. The absolute diffusion coefficients lie in the range (1.25–2.70)

Table 2 Dye diffusion coefficients and depth of penetration (1% of surface concentration) into various acceptor polymers

Acceptor polymer	T_g (°C)	Diffusion coeff. (10^{-7} cm^2 s^{-1})	Penetration depth (μm)
A	47	2.70 ± 0.79	2.12 ± 0.31
B	67	2.24 ± 0.66	1.94 ± 0.29
C	71	1.66 ± 0.49	1.67 ± 0.25
D	85	1.56 ± 0.31	1.62 ± 0.16
E	100	1.25 ± 0.67	1.45 ± 0.40

$\times 10^{-7}$ cm^2 s^{-1}. Hann and Beck[1] determined diffusion coefficients for thermal transfer printing dyes in polyesters with T_g in the range 67–100°C. Typical diffusion coefficients were found to vary from approximately 5×10^{-10} cm^2 s^{-1} at 100°C to 5×10^{-6} cm^2 s^{-1} at 240°C. These experiments were performed at constant temperature. It can be seen that the diffusion coefficients determined from the RBS profiles are of the same order as but slightly lower than those obtained by Hann and Beck. However, the dye diffusion profiles are created using a thermal transfer printer with a non-isothermal diffusion step and a maximum temperature of approximately 250–300°C. Considering that the diffusion coefficient obtained from the RBS profile is an average value over a range of temperatures, the agreement with the isothermal work of Hann and Beck is reasonable.

Relation of dye diffusion results to solute diffusion theory

There have been many studies of the permeability and diffusion of solutes in polymer matrices. Distinctions have been made between small molecules (gases) and large molecules (liquids and vapours) that interact strongly with the polymer[15]. It is generally accepted that, for translational motion of a solute to occur, a space of sufficient size must exist into which the solute molecule can move. Therefore, small molecules will readily permeate through glassy polymers provided they are soluble. Larger molecules, comparable to or larger than the polymer repeat unit, require a cooperative movement of several polymer segments to create a large enough space for diffusion to occur, and their diffusion rates are therefore coupled to the polymer relaxation processes[16]. These processes are extremely slow in the glassy state below T_g but become rapid in the rubbery state above T_g (ref. 17) and explain the large step observed in the diffusion coefficients at T_g (ref. 18). In the work reported here, we investigate the diffusion of a solute with a molecular weight of 340 in amorphous polymers above T_g. The solute molecular weight is 3–4 times greater than that of the polymer repeat units and interacts well with the acceptor (*Table 1* shows that the dye and polymer solubility parameters are closely matched). This explains why the calculated diffusion coefficients and depths of penetration are strongly linked to the glass transition temperature of the acceptor matrix.

Many studies have tried to quantify this dependence in terms of free-volume interpretations[19–26] from which the Williams–Landel–Ferry (WLF) equation is derived[27]:

$$\log(a_T) = C_1(T - T_g)/(C_2 + T - T_g) \qquad (3)$$

where C_1 and C_2 are polymer-dependent constants and a_T is the transport coefficient, which is dependent on the system studied and here taken to be[28]: D/D_g. The value of C_2 is often considered to be polymer-independent with a value of 51.6°C, and equation (3) can be rewritten as:

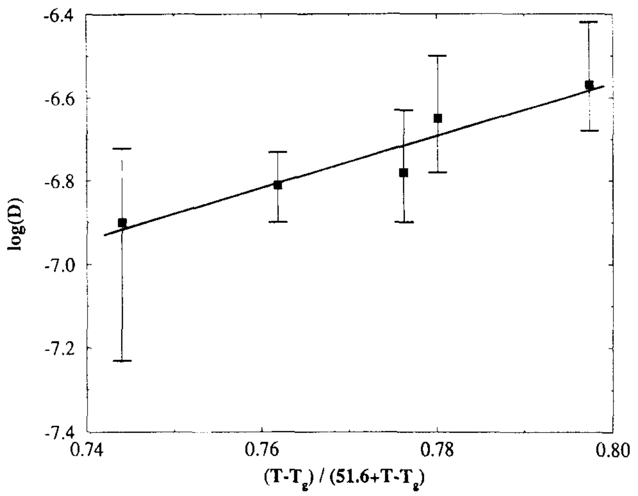

Figure 4 The comparison of dye diffusion coefficients to the free-volume theory, according to the WLF equation. The data were plotted according to equation (4) where D is the diffusion coefficient determined by RBS, T is the transfer temperature modelled as 250°C and T_g is the glass transition temperature of the acceptor polymer matrix

$$\log(D) = C_1(T - T_g)/(51.6 + T - T_g) + \log(D_g) \qquad (4)$$

As described earlier, all polymers have similar compositions (mixtures of the same polymers in varying quantities) and we therefore assume that their only physical difference is their T_g. In this way the WLF equation can be used with average values for C_1 and D_g and using T_g as the variable. *Figure 4* shows a plot of $\log(D)$ against $(T - T_g)/(51.6 + T - T_g)$, where $T = 523$ K is the average temperature of printing determined from Hann and Beck's modelling work[1]. The slope of the best straight-line fit (shown in *Figure 4*) gives an average value of C_1 for the five polymers used and is found to be $\overline{C_1} = 6.24$. This is comparable to many of the values tabulated in Ferry[27] for a wide range of polymers. The intercept of the fit with the y-axis yields the average value of D_g (the diffusion coefficient at $T = T_g$), which is found to be: $\overline{D_g} = 2.76 \times 10^{-12}$ cm^2 s^{-1}.

The Doolittle equation[29] (from which the WLF equation is derived) assumes that $T_g < T < (T_g + 100)$. In the thermal transfer printing and at the print times used, $T - T_g$ varies between approximately 150 and 200°C (assuming the average temperature of printing to be 250°C). *Figure 4* shows that our data agree with a free-volume interpretation despite $T - T_g$ falling outside the range usually associated with the Doolittle and WLF equations. This is probably due to the somewhat arbitrary limit of $T_g + 100$, which does not represent any physical boundary, but broadly defines the region in which the viscoelastic friction coefficient is non-linear. Any deviations from the WLF predictions above $T_g + 100$ are therefore expected to occur slowly, showing no discontinuities.

The analysis of dye transport as being solely controlled by free volume is, to a certain extent, a simplification. As previously mentioned, dye transport during thermal transfer printing can be considered as a permeability from a donor to an acceptor polymer matrix. From the solution/diffusion model of permeability[30], the permeability is given by:

$$P = DS \tag{5}$$

where P, D and S are the coefficients of permeability, diffusivity and solubility, respectively. The solubility coefficient is given by:

$$S = S_0 \exp(-\Delta H/RT) \tag{6}$$

where ΔH is the heat of mixing between two components, which is defined by[31]:

$$\Delta H = \Phi_d \Phi_p (\delta_d - \delta_p)^2 \tag{7}$$

where Φ_d and Φ_p are the volume fractions and δ_d and δ_p are the solubilities of the dye and polymer, respectively. Combining equations (6) and (7) with the solubilities shown in *Table 1* (with errors of 1 $(\mathrm{J\,cm^{-3}})^{1/2}$ (ref. 32)) shows that, within experimental error, S is constant for all the polymers used here. The permeability is then directly proportional to the diffusivity and the dye transport is adequately described by diffusion coefficients alone.

Absolute dye concentrations

In order to obtain absolute concentrations, a detailed knowledge of the atomic composition of both the dye molecule and the acceptor polymer are required. The RBS spectra are analysed using the program RUMP[33,34]. Initial simulations of the spectra are obtained for theoretical samples of pure acceptor polymer (i.e. without dye). Reasonable fits are usually obtained. Sulfur is then added to these theoretical spectra until the simulated sulfur edge matches the experimental data. This sulfur content enables calculation of the corresponding dye content from knowledge of the atomic composition of the dye. Corrections are then made to the overall composition of the theoretical samples to account for the presence of the remainder of the dye molecule. *Figure 5* shows an example of a simulation, and *Table 3* summarizes the results obtained, where the dye concentrations are given as mass fractions, $M_{\mathrm{dye}}/M_{\mathrm{matrix}}$. These concentrations are for the sample surface only because the simulation program used does not permit the modelling of substances of varying concentration with depth. The concentration at depth is then calculated using equation (2) normalized to the surface concentration. The values reported in *Table 3* show only slight fluctuations around a mean value of 0.161. These fluctuations do not appear to be correlated to the polymer T_g and are thought to be dependent only on the initial dye concentration in the donor ribbon.

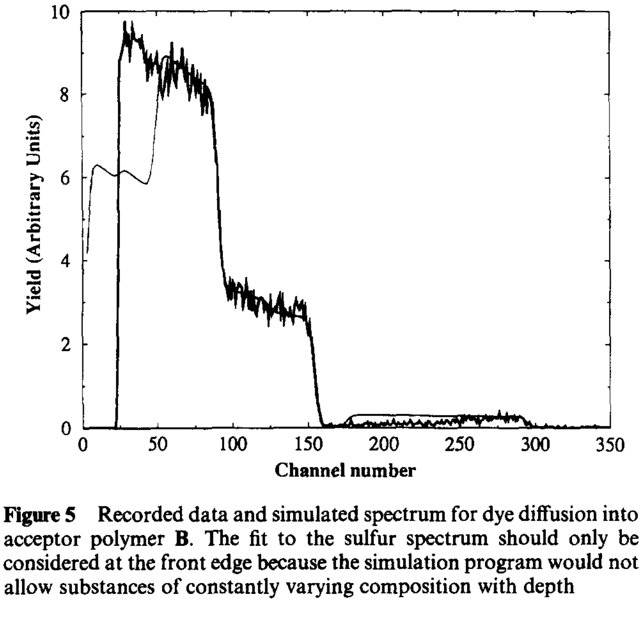

Figure 5 Recorded data and simulated spectrum for dye diffusion into acceptor polymer **B**. The fit to the sulfur spectrum should only be considered at the front edge because the simulation program would not allow substances of constantly varying composition with depth

Table 3 Average dye concentration at sample surfaces obtained by simulation

Acceptor polymer	T_g (°C)	$M_{\mathrm{dye}}/M_{\mathrm{matrix}}$
A	47	0.157
B	67	0.170
C	71	0.156
D	85	0.143
E	100	0.181

SUMMARY

The Rutherford backscattering ion-beam technique is a method sufficiently accurate, reliable and sensitive to allow the study of diffusion of a sulfur-labelled dye into (C,H,O) polymers where the dye penetrates the polymer to a depth of a few micrometres.

Thermal transfer printing was used to transfer a heterocylic azo dye into acceptor polymers of varying glass transition temperature. The dye concentration was highest at the surface and fell to zero within a distance of 1–2 μm depending on the T_g of the acceptor matrix. The solute profiles were fitted with error-function models to obtain diffusion coefficients that showed a strong dependence on the T_g of the acceptor matrix. The coupling of diffusivity to the relaxation process was explained in terms of solute molecular size relative to the polymer repeat units and of solute–polymer interactions.

The diffusion coefficients correlated well with free-volume interpretations of solute diffusion by agreeing with the WLF equation. Solubility parameters showed that dye–polymer interactions were similar for all the polymers studied.

Absolute dye concentrations were obtained via simulation and the mass fraction of dye at the surface of the matrix was found to be in the range 0.143–0.181.

ACKNOWLEDGEMENTS

The authors wish to thank Alan Butters from ICI Imagedata for several useful discussions and wish to thank ICI Imagedata for funding the use of the Van de Graaff Accelerator at the University of Surrey.

REFERENCES

1 Hann, R. A. and Beck, N. C. *J. Imaging Technol.* 1990, **16**, 238
2 Hann, R. A. 'Imaging Science and Technology', 8th Int. Congress on Advances in Non-Impact Printing Technologies, 1992
3 Shinozaki, K. and Hirano, H. *J. Imaging Sci. Technol.* 1994, **38**(6), 571
4 Allen, G. and Bevington, J. C. (Eds.) 'Comprehensive Polymer Science', Pergamon Press, Oxford, 1989, Vol. 1, Ch. 24
5 Harrick, N. J. 'International Reflection Spectroscopy', Harrick Scientific, 1967
6 Richards, R. W. and Penfold, J. *Trends Polym. Sci.* 1994, **2**(1), 5

7 Chu, W., Mayer, J. W. and Nicolet, M. 'Backscattering Spectrometry', Academic Press, New York, 1965

8 Fedors, R. F. *Polym. Eng. Sci.* 1974, **14**, 147

9 Van Krevelen, D. W. 'Properties of Polymers', Elsevier Science, Amsterdam, 1986

10 Marrion, J. B. 'Classical Dynamics of Particles and Systems', Oxford University Press, Oxford, 1991

11 Williams, W. S. C. 'Nuclear and Particle Physics', Oxford University Press, Oxford, 1991

12 Ziegler, J. F. and Biersack, J. P. 'TRIM: The Stopping and Range of Ions in Solids', Pergamon Press, Oxford, 1985

13 Ziegler, J. F., Biersack, J. P. and Littmark, U. 'The Stopping and Range of Ions in Matter', Pergamon Press, Oxford, 1985

14 Crank, J. 'The Mathematics of Diffusion', Oxford University Press, Oxford, 1975

15 Stannet, V. 'Diffusion in Polymers' (Eds J. Crank and G. S. Park), Academic Press, New York, 1968, Ch. 2

16 Kumins, C. A. and Kwei, T. K. 'Diffusion in Polymers' (Eds J. Crank and G. S. Park), Academic Press, New York, 1968, Ch. 4

17 Fujita, H. 'Diffusion in Polymers' (Eds J. Crank and G. S. Park), Academic Press, New York, 1968, Ch. 3

18 Stern, S. A. and Trohalaki, S. 'Barrier Polymers and Structures' (Ed. W. J. Koros), ACS Symposium Series 423, American Chemical Society, Washington, DC, 1990, Ch. 2

19 Bueche, F. *J. Chem. Phys.* 1953, **21**, 1850

20 Ferry, J. D. 'Viscoelastic Properties of Polymers', 2nd Edn., Wiley, New York, 1970

21 Fujita, H. *Fortschr. Hochpolym. Forsch.* 1961, **3**, 1; Fujita, H., Kishimoto, A. and Matsumoto, K. *Trans. Faraday Soc.* 1960, **56**, 424

22 Cohen, M. H. and Turnbull, D. *J. Chem. Phys.* 1959, **31**, 1164

23 Vrentas, J. S. and Duda, J. L. *J. Polym. Sci., Polym. Phys. Edn.* 1977, **15**, 403; *Macromolecules* 1976, **9**, 785

24 Vrentas, J. S. and Duda, J. L. in 'Encyclopaedia of Polymer Science and Engineering', Wiley, New York, 1986, Vol. 5

25 Mauritz, K. A., Storey, R. F. and George, S. E. *Macromolecules* 1990, **23**, 441

26 Coughlin, C. S., Mauritz, K. A. and Storey, R. F. *Polym. Mater. Sci.* 1989, **61**, 171

27 Williams, M. L., Landel, R. F. and Ferry, J. D. *J. Am. Chem. Soc.* 1955, **77**, 3701

28 Chen, S. P. and Ferry, J. D. *Macromolecules* 1968, **1**, 270

29 Doolittle, A. K. *J. Appl. Phys.* 1951, **22**, 1471

30 dev Naylor, T. 'Comprehensive Polymer Science' (Eds G. Allen and J. C. Bevington), Pergamon Press, Oxford, 1989, Vol. 2, Ch. 2

31 Hildebrand, J. H., Prausnitz, J. M. and Scott, R. L. 'Regular and Related Solutions', Van Nostrand Reinhold, New York, 1970

32 Coleman, M. M., Graf, J. F. and Painter, P. C. 'Specific Interactions and the Miscibility of Polymer Blends', Technomic, Lancaster, PA, 1991

33 Doolittle, L. R. *Nucl. Instrum. Meth. (B)* 1985, **9**, 344

34 Doolittle, L. R. *Nucl. Instrum. Meth (B)* 1986, **15**, 227